

RESEARCH

Open Access



# Morphological characterization of atypical pancreatic ductal adenocarcinoma with cystic lesion on DCE-CT: a comprehensive retrospective study

Jing Chen<sup>1</sup>, Qi Wu<sup>2</sup>, Ling Liu<sup>1</sup>, Yuan Yuan<sup>2</sup>, Shengsheng Lai<sup>3</sup>, Zhe Wu<sup>4</sup> and Ruimeng Yang<sup>4\*</sup> 

## Abstract

**Background** Pancreatic ductal adenocarcinoma (PDAC) with cystic features presents significant challenges in achieving an accurate preoperative diagnosis and in implementing appropriate clinical management. The aim of this study was to analyze the dynamic contrast-enhanced computed tomography (DCE-CT) findings of PDACs with cystic lesions and correlate them with histopathological findings.

**Methods** We retrospectively reviewed 40 patients with pathology-proven PDACs exhibiting cystic lesions who underwent preoperative DCE-CT imaging. The CT manifestations were classified into three subtypes based on the morphological characteristics of the cystic lesions: Type 1, small proportion (< 50%) of intratumoral cystic lesions, with or without associated peritumoral cystic lesions; Type 2, large proportion ( $\geq$  50%) of intratumoral cystic lesions, with or without associated peritumoral cystic lesions; Type 3, a solid pancreatic mass with accompanying peritumoral cystic lesions. The DCE-CT findings were analyzed based on location, size, contour, enhancement patterns, and secondary findings, and compared with the corresponding pathological diagnoses.

**Results** Among the 40 patients, 23 (57.5%) tumors were located in the pancreatic body or tail. Type 1 was identified in 21 cases, Type 2 in 6 cases, and Type 3 in 13 cases. All masses exhibited a bulging pancreatic contour, with 4 cases showing isoattenuating enhancement on DCE-CT. Secondary signs were present in 87.5% (35/40) of cases. Notably, 15 cases (37.5%) were misdiagnosed or missed. Surgical resection specimens demonstrated common pathological features, including large duct-like cysts and coagulative necrosis.

**Conclusion** Atypical PDAC with cystic lesions is a relatively uncommon variant that exhibits a range of DCE-CT features, along with distinct pathological characteristics. Familiarity with these imaging features is essential for radiologists in order to minimize the risk of misdiagnosis and guide appropriate clinical management of these challenging cases.

\*Correspondence:

Ruimeng Yang  
eyruimengyang@scut.edu.cn

<sup>1</sup>Department of Radiology, the First College of Clinical Medical Science, China Three Gorges University, Yichang Central People's Hospital, Yichang, China

<sup>2</sup>Department of Pathology, the First College of Clinical Medical Science, China Three Gorges University, Yichang Central People's Hospital, Yichang, China

<sup>3</sup>School of Medical Equipment, Guangdong Food and Drug Vocational College, Guangzhou, Guangdong, China

<sup>4</sup>Department of Radiology, the Second Affiliated Hospital, School of Medicine, South China University of Technology, Guangzhou, Guangdong, China



© The Author(s) 2025. **Open Access** This article is licensed under a Creative Commons Attribution-NonCommercial-NoDerivatives 4.0 International License, which permits any non-commercial use, sharing, distribution and reproduction in any medium or format, as long as you give appropriate credit to the original author(s) and the source, provide a link to the Creative Commons licence, and indicate if you modified the licensed material. You do not have permission under this licence to share adapted material derived from this article or parts of it. The images or other third party material in this article are included in the article's Creative Commons licence, unless indicated otherwise in a credit line to the material. If material is not included in the article's Creative Commons licence and your intended use is not permitted by statutory regulation or exceeds the permitted use, you will need to obtain permission directly from the copyright holder. To view a copy of this licence, visit <http://creativecommons.org/licenses/by-nc-nd/4.0/>.

## Introduction

Pancreatic ductal adenocarcinoma (PDAC) is a highly aggressive malignancy with a poor prognosis, marked by a dismal 5-year survival rate of less than 9% [1, 2]. Imaging techniques, including computed tomography (CT) and magnetic resonance (MR) imaging, are crucial in the detection and staging of PDAC, with CT being the primary modality for providing reliable morphological information to assist in diagnosis. While most PDACs exhibit typical CT features of solid and hypovascular masses, some present with atypical imaging characteristics, including cystic features [3]. The presence of “cystic” components can lead to missed diagnoses of PDAC or misdiagnosis due to their overlap with other pancreatic cystic tumors, thus posing significant challenges to preoperative diagnosis and clinical management [4].

Kosmahl et al. [5] in a 2005 study were the first to classify cystic lesions of PDACs from a perspective of pathology into four categories: (i) large duct-like cysts lined by atypical cuboidal or flat epithelial cells; (ii) degenerative cystic changes with necrotic and hemorrhagic tissue; (iii) retention cysts due to duct obstruction from the tumor; and (iv) pseudocysts resulting from tumor-related pancreatitis. Subsequent radiological-pathological studies have revealed additional presentations of cystic PDACs, including multiple large neoplastic cysts with dysplastic or malignant epithelium lining the cyst walls [6, 7], intratumoral neoplastic cysts lined by mucin-producing neoplastic cells surrounded by the fibrous stroma of typical PDACs [8, 9], and large-duct variants characterized by microcystic and papillary patterns on pathology [10–12]. Cystic changes in pancreatic cancer are rare and exhibit a wide range of origins and morphological variations. However, previous studies have primarily focused on (i) pathological studies of PDACs with cystic changes, and (ii) case reports or studies that primarily use MRI to examine specific cystic pathological changes in PDAC [11, 13]. There is currently no comprehensive, systematic report on the CT imaging features of PDACs with cystic lesions.

Therefore, this retrospective study aims to systematically analyze and summarize the DCE-CT morphological features of PDACs with cystic lesions, and explore their associated clinicopathological characteristics. The findings aim to improve the understanding of PDACs with atypical CT presentations, reduce the risk of diagnostic misinterpretation, and facilitate more accurate diagnostic practices.

## Materials and methods

### Study population

This retrospective study was approved by the Ethics Committee of Yichang Central People’s Hospital. Due to the retrospective nature of the study, the requirement for

written informed consent was waived. A total of 257 consecutive patients with pathologically confirmed PDAC were identified from the hospital’s pathology database between January 2016 and June 2023. The inclusion criteria were as follows: (1) presence of cystic lesions on CT imaging; (2) DCE-CT data obtained within two weeks prior to surgery or biopsy. Exclusion criteria were: (1) insufficient preoperative radiological data; (2) cystic lesions less than 5 mm or with poorly defined margins; (3) prior preoperative treatment; (4) imaging features suggestive of chronic pancreatitis, which is associated with a higher incidence of pseudocysts; (5) co-existing pancreatic cystic neoplasms. Following these criteria, 40 patients were ultimately included in this study. A flow diagram of the patient inclusion process is shown in Fig. 1.

### CT protocol

All abdominal CT examinations were performed using the following scanners: SOMATOM Definition Flash (Siemens Healthcare), Toshiba Aquilion 320 (Toshiba Medical Systems), and LightSpeed VCT 64 (GE Healthcare). Imaging parameters were as follows: tube voltage of 120 kV, tube current-time product of 150–300 mA, or automated tube current modulation (200–400 mA), with a noise index section and a slice thickness of 1–5 mm, matrix of 512 × 512. For the DCE-CT acquisition, a non-ionic contrast agent with iodine concentrations ranging from 300 to 350 mg/mL was injected intravenously at a rate of 2.5–3.5 mL/s and a dose of 1.5 mL/kg. Imaging was performed at three phases: pancreatic phase (35–40 s), portal venous phase (65–70 s), and delayed phase (180–300 s).

### Image analysis

#### CT classification criteria

Cystic lesions in PDACs were classified according to the following criteria: (1) no enhancement in all DCE-CT phases; (2) the average CT value of the region of interest (ROI) was between –10 HU and 20 HU [14], and the ROI occupied at least half of the cystic area; (3) measurements and evaluations were performed using axial images from the delayed phase; (4) the cystic lesion had a short diameter greater than 5 mm with well-defined margins. Based on these features, atypical PDACs with cystic lesions were classified into three subtypes based on their morphological characteristics: **Type 1**, Small intratumoral cystic lesions (proportion of cystic components < 50%), with or without peritumoral cystic lesions; **Type 2**, Large intratumoral cystic lesions (proportion of cystic components ≥ 50%), with or without peritumoral cystic lesions; **Type 3**, Solid pancreatic mass with peritumoral cystic lesions. A schematic illustration of these three subtypes is shown in Fig. 2.

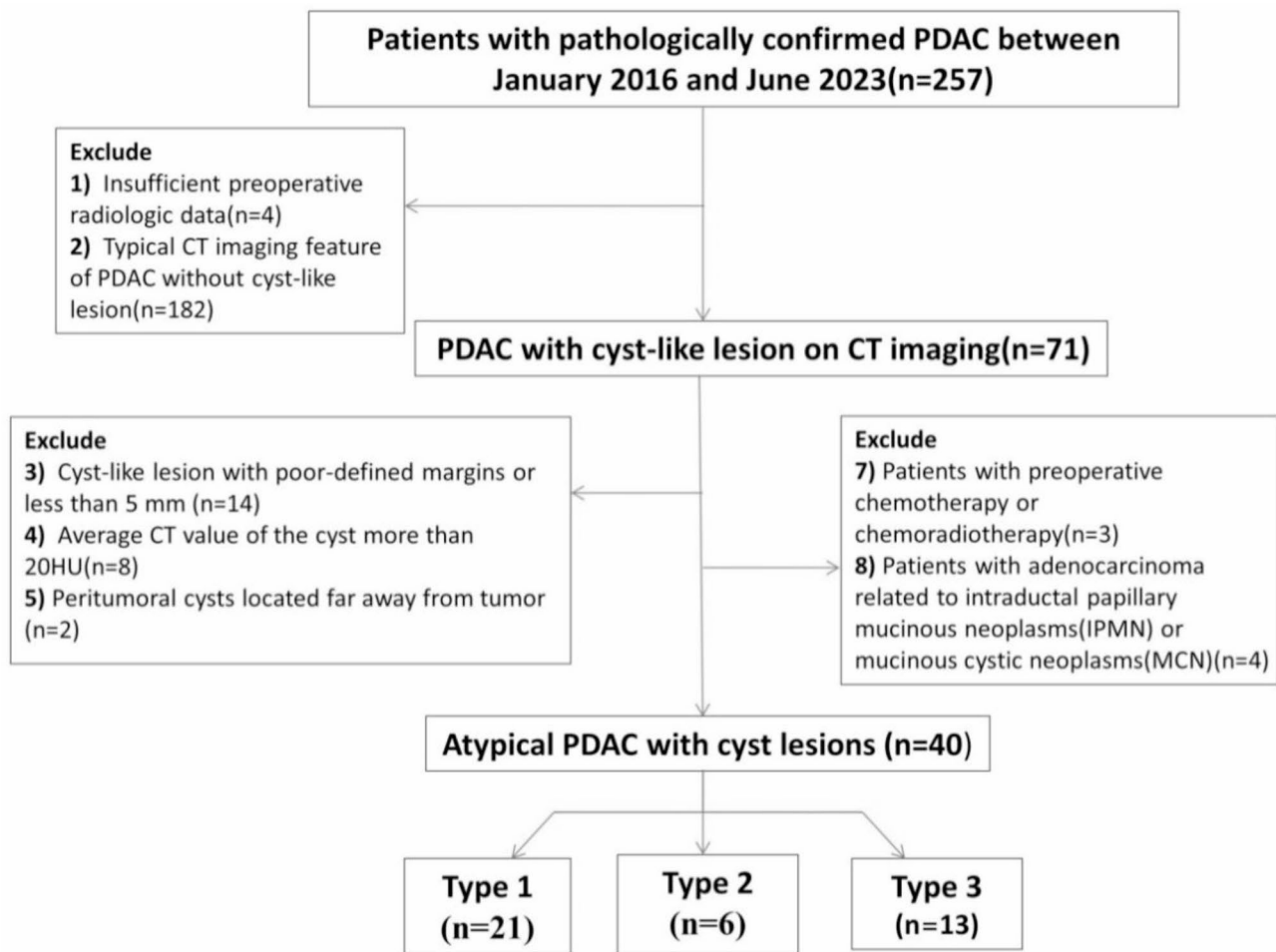


**Fig. 1** The patient inclusion flowchart

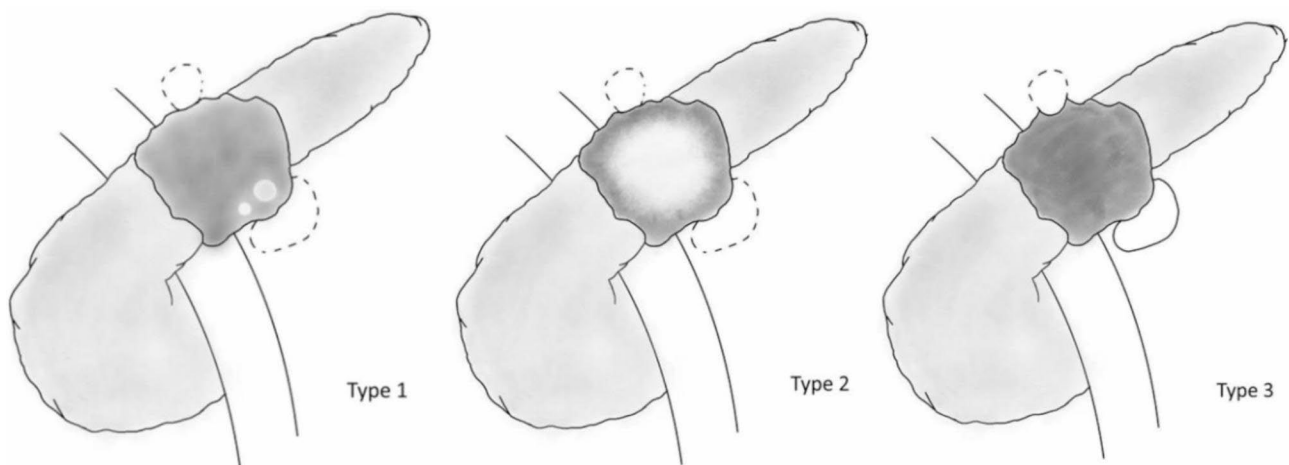


**Fig. 2** Schematic of atypical PDAC with cystic lesions: **Type 1** features small intratumoral cystic lesions, with cystic component comprising < 50% of the tumor, with or without peritumoral cystic lesion; **Type 2** is characterized by large intratumoral cystic lesions, with the cystic component accounting for  $\geq 50\%$  of the tumor, with or without peritumoral cystic lesion. **Type 3** presents as a solid mass within the pancreatic parenchyma, accompanied by peritumoral cystic lesion

### CT imaging evaluation

CT imaging features were evaluated based on the following parameters: tumor subtype (according to the classification criteria outlined in this study); tumor location (head/uncinate or body/tail, based on their location relative to the superior mesenteric vein); tumor contour (bulging or not), tumor size (maximal axial dimension in the pancreatic phase); cystic lesion characteristics (location, number, and size, with the largest lesion being measured if multiple cystic lesions were present); tumor attenuation on DCE-CT (hypoattenuating masses or nodules in the pancreatic parenchymal phase, isoattenuating lesions in both the pancreatic and portal venous phases [15]); Secondary signs, including pancreatic duct abnormalities (e.g., abrupt cutoff, or upstream dilatation of the main pancreatic duct, with the diameter exceeded 3 mm at the pancreatic head and 2 mm in the body and tail), biliary tree abnormalities (e.g., abrupt cutoff, or upstream dilatation, with a diameter greater than 9 mm), and upstream pancreatic parenchymal atrophy (defined as subjective narrowing of the parenchyma compared with both upstream and downstream surrounding tissue, unless atrophy was confined to the edge of the pancreas, in which case it was compared with adjacent parenchyma on one side [16]), were also assessed; vascular invasion (including abutment, encasement, occlusion, and tumor thrombosis) was evaluated; peripancreatic organ invasion or distant metastases (metastasis to lymph nodes outside the typical drainage pathways was included) were considered. All DCE-CT images of PDACs with cystic lesions were independently reviewed by two experienced radiologists. The radiologists were blinded to the final diagnosis but were informed that the individuals included in the study cohort were suspected to have PDAC. Discrepancies in interpretation were resolved by consensus. To assess interobserver agreement, we performed Cohen's kappa ( $\kappa$ ) statistics to assess interobserver agreement for morphological classification and primary CT features interpretation. The agreement levels were categorized according to the Landis and Koch criteria: 0.81–1.00 as almost perfect, 0.61–0.80 as substantial, and 0.41–0.60 as moderate, 0.21–0.40 as fair, and <0.20 as poor agreement.

### Histopathologic analysis

Histopathological materials including digital reports and H&E staining specimen slices from all 23 patients underwent surgical resection were retrospectively reviewed by a gastrointestinal pathologist at our institution. The histopathological reports and gross specimen photographs of all patients were thoroughly examined. Pathological features from the 23 surgical resections were assessed, including tumor size, TNM staging [17], histological differentiation grading (well-differentiated, moderately differentiated, or poorly differentiated), and evidence of

direct peripancreatic infiltration (perineural invasion and peripancreatic fat involvement) were assessed. Additionally, the pathologist identified cystic structures in both macroscopic and microscopic examinations, noting features such as large duct-type cysts, coagulative necrosis, cystic degeneration, and extracellular mucin deposits.

## Result

### Patient characteristics

This study included 40 patients diagnosed with PDACs, consisting of 22 men and 18 women, aged between 42 and 91 years, with a mean age of  $60.4 \pm 10.2$  years. Of these patients, 5 had preoperative carbohydrate antigen 19–9 (CA 19–9) levels below 37 U/mL, while the remaining 35 patients had CA 19–9 levels  $\geq 37$  U/mL. In this cohort, 23 patients underwent surgical resection and were pathologically confirmed, while 17 patients were confirmed through endoscopic ultrasound-guided fine-needle aspiration (EUS-FNA) or histological biopsy.

### CT findings

The interobserver agreement for morphological classification and interpretation of primary CT features between the two radiologists was quantitatively assessed using a simple  $\kappa$  analysis. The analysis revealed excellent interobserver agreement for most imaging characteristics, including morphological classification ( $\kappa=0.876$ ), pancreatic parenchymal atrophy ( $\kappa=0.948$ ), pancreatic duct abnormalities ( $\kappa=1.00$ ), and biliary tree abnormalities ( $\kappa=1.00$ ). Substantial agreement was observed for peripancreatic organ invasion or distant metastases ( $\kappa=0.781$ ), vascular invasion ( $\kappa=0.754$ ), and enhancement patterns ( $\kappa=0.722$ ).

Among the 40 patients, 23 (57.5%) were predominantly located in the body/tail of the pancreas. Most patients (90%) exhibited hypoattenuation on DCE-CT. All patients demonstrated bulging contours with lobulated or irregular shapes, consistent with expansive or exophytic growth patterns (100%). The mean tumor size was 4.9 cm (range 1.5–13.5 cm). Secondary signs were present in 87.5% of cases (35/40). One case (2.5%) was missed, and 14 cases (35%) were misdiagnosed (Table 1).

**Type 1** was observed in 21 patients (52.5%), where intratumoral cystic lesions were eccentrically located, ranging from 1 to 5 cysts, with the proportion of cystic components being less than 50% (as shown in Figs. 3a and 3b). Peritumoral cystic lesions were seen in 5 patients, with a mean maximal diameter of 2.1 cm (range 0.9–3.6 cm) as shown in Figs. 3c and 3d. One patient exhibited isoattenuating enhancement on DCE-CT. 7 cases involved adjacent organs. Liver metastasis was detected in 5 patients. **Type 2** atypical PDACs with cystic lesions occurred in 6 patients (15%), characterized by 1 to 2 intratumoral cystic

**Table 1** Clinical and dynamic contrast-enhanced CT imaging characteristics of pancreatic adenocarcinomas with cystic lesions

Variables	Total (n=40)	Type1 (n=21)	Type 2 (n=6)	Type3 (n=13)
Mean age (y)*	60.4±10.2	59.1±8.4	58.5±9.8	63.3±12.9
Sex				
male	22 (55%)	9(42.9%)	4 (66.7%)	9 (69.2%)
female	18(45%)	12 (57.1%)	2 (33.3%)	4 (30.8%)
CA199				
<37 U/mL	5 (12.5%)	2 (9.6%)	1 (16.7%)	2 (15.4%)
≥37 U/mL	35 (87.5%)	19 (90.4%)	5 (83.3%)	11 (84.6%)
Size (cm)†	4.3 (3.2, 5.6)	4.1 (3.2, 5.2)	5.4 (3.9, 6.3)	3.9 (2.8, 5.8)
Location				
head/uncinate	11 (27.5%)	6 (28.6%)	1 (16.7%)	4 (30.8%)
body/ tail	23 (57.5%)	11 (52.4%)	4 (66.7%)	8 (61.5%)
simultaneously involved	6 (15%)	4 (19.0%)	1 (16.7%)	1 (7.7%)
Tumor Contour bulging				
Absence	0(0)	0(0)	0(0)	0(0)
Presence	40 (100%)	21 (100%)	6 (100%)	13 (100%)
Enhancement pattern on DCE-CT				
isoattenuating	4 (10%)	1 (4.8%)	1 (16.7%)	2 (15.4%)
hypoattenuating	36 (90%)	20 (95.2%)	5 (83.3%)	11 (84.6%)
Secondary signs&	35 (87.5%)	19(90.5%)	5 (83.3%)	11(84.6%)
pancreatic duct abnormalities	34 (85%)	19 (90.5%)	5 (83.3%)	10 (76.9%)
biliary tree abnormalities	10 (25%)	6 (28.6%)	0 (0)	4 (30.8%)
pancreatic parenchymal atrophy	24 (60%)	13(61.9%)	3 (50%)	8 (61.5%)
vascular invasion	31 (77.5%)	16 (76.2%)	6 (100%)	9 (69.2%)
peripancreatic organ invasion or distant metastases	24(60%)	11(52.4%)	6(100%)	7(50%)
Missed diagnosis	1 (2.5%)	1 (5%)	0 (0)	0 (0)
Misinterpreted diagnosis	14 (35%)	4 (19%)	5 (83.3%)	5 (38.5%)

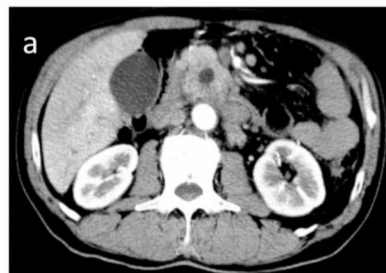
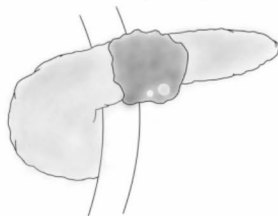
Note—Except for age and size, Data are in number of occurrences. Data in parentheses represent percentages

\*Data are expressed as mean ± standard deviation

†Data are expressed as median (IQR, 1st to 3rd quartile)

&any Secondary sign indicates positivity

**Type 1 without peritumoral cystic lesion (n=16)**



**Type 1 with peritumoral cystic lesion (n=5)**

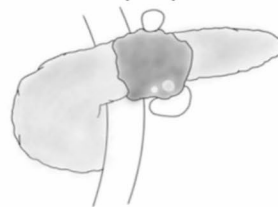
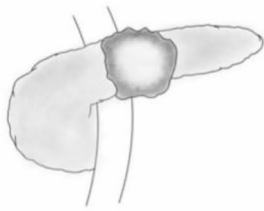


**Fig. 3** CT morphology of PDAC with cystic lesions: **a, b** Type 1 without peritumoral cystic lesions in two different patients. **c, d** Type 1 with multiple peritumoral cystic lesions in the same patient

**Type 2 without peritumoral cystic lesion  
(n=4)**



**Type 2 with peritumoral cystic lesion  
(n=2)**

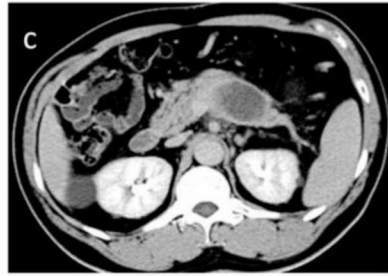
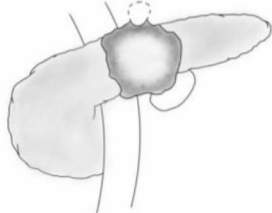
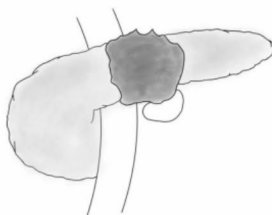


**Fig. 4** CT morphology of PDAC with cystic lesions: **a, b** Type 2 without peritumoral cystic lesions in two different patients. **c, d** Type 2 with peritumoral cystic lesions in the same patient

**Type 3 with mono-peritumoral cystic lesion  
(n=6)**



**Type 3 with multi-peritumoral cystic lesion  
(n=7)**

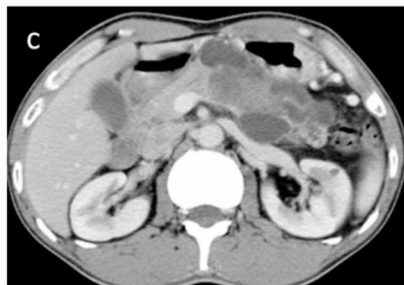
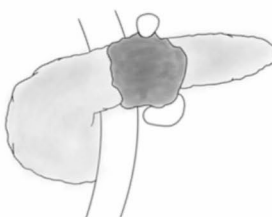


**Fig. 5** CT morphology of PDAC with cystic lesions: **a, b** Type 3 with a single peritumoral cystic lesion in two different patients. **c, d** Type 3 with multiple peritumoral cystic lesions in the same patient

lesions, where cystic components comprised  $\geq 50\%$  of the tumor, as shown in Figs. 4a-4c. Two of these patients presented with a peritumoral cyst as shown in Fig. 4d. The mean cyst diameters were 1.4 cm and 3 cm, respectively. One patient showed isoattenuating enhancement on DCE-CT. 3 cases involved adjacent organs. Distant metastasis was observed in 4 patients,

with 3 of these patients developing liver metastasis and 1 metastasizing to mesenteric lymph nodes. **Type 3** solid PDACs with peritumoral cystic lesions were seen in 13 patients (32.5%), where the number of cysts ranged from 1 to 7, with a mean maximal diameter of 3.3 cm (range 0.9–5.6 cm), as shown in Fig. 5a-5d. Two patients exhibited isoattenuating enhancement

on DCE-CT. 3 cases involved adjacent organs. Distant metastases were detected in 7 patients, including 2 with liver metastasis and 5 with metastasis to lymph nodes outside the common drainage pathways or omental invasion.

### Pathological findings

Among 23 surgically resected cases, 14 PDACs (60.9%) were moderately differentiated, while 9 PDACs (39.1%) were poorly differentiated. Peripancreatic perineural invasion was observed in 19 cases (82.6%), and fat invasion was present in 14 cases (60.9%). Macroscopically, 15 cases (65.2%) exhibited visually cyst-like cavities (Fig. 6b and e). Microscopically, 14 cases (60.9%) exhibited visually cyst-appearing lesions, 6 cases showed large duct-type features (Fig. 6c), including 1 case featured extracellular mucin deposits. 6 cases exhibited coagulative necrosis (Fig. 6f). 2 cases featured extracellular mucin deposits. (Table 2).

Additionally, as indicated in Supplemental Table 1, the rate of fat invasion in PDACs with peritumoral cystic lesions was significantly higher than in those without peritumoral cysts (90.9% vs. 36.3%). Furthermore, moderately differentiated PDACs were more common in cases with peritumoral cystic lesions compared to those without peritumoral cysts (83.3% vs. 36.3%).

### Discussion

PDAC typically presents as solid tumor, however, it may occasionally exhibit cystic components, which can lead to diagnostic confusion with pancreatic cystic neoplasms on imaging. Despite significant advancements in imaging techniques for PDAC, the diagnosis of PDAC with cystic lesions remains challenging. This is primarily due to the lack of a clear definition of cystic changes and insufficient recognition of cystic degeneration in PDACs. In this study, we proposed a CT-based morphological classification system for PDACs with cystic lesions, categorizing them into three subtypes. This classification system showed excellent interobserver agreement ( $\kappa=0.876$ ) among different radiologists. The prevalence of PDACs with cystic components is low, accounting for approximately 1–8% of PDAC cases according to previous studies [5, 8, 9, 12, 18–21]. In our cohort of 257 PDAC patients, the incidence of PDAC with cystic lesions confirmed by surgical resection pathology was 8.9% (23/257), consistent with previously reported rates. Unlike conventional PDACs, which typically occur in the pancreatic head, we found that the majority of PDACs with cystic lesions (57.5%) were located in the pancreatic body/tail. Type 1, characterized by small intratumoral cystic lesions, was the most common subtype in our study, accounting for 52.5% (21/40) of cases. Notably, PDACs with cystic lesions can closely mimic pancreatic cystic neoplasms on imaging [22, 23].

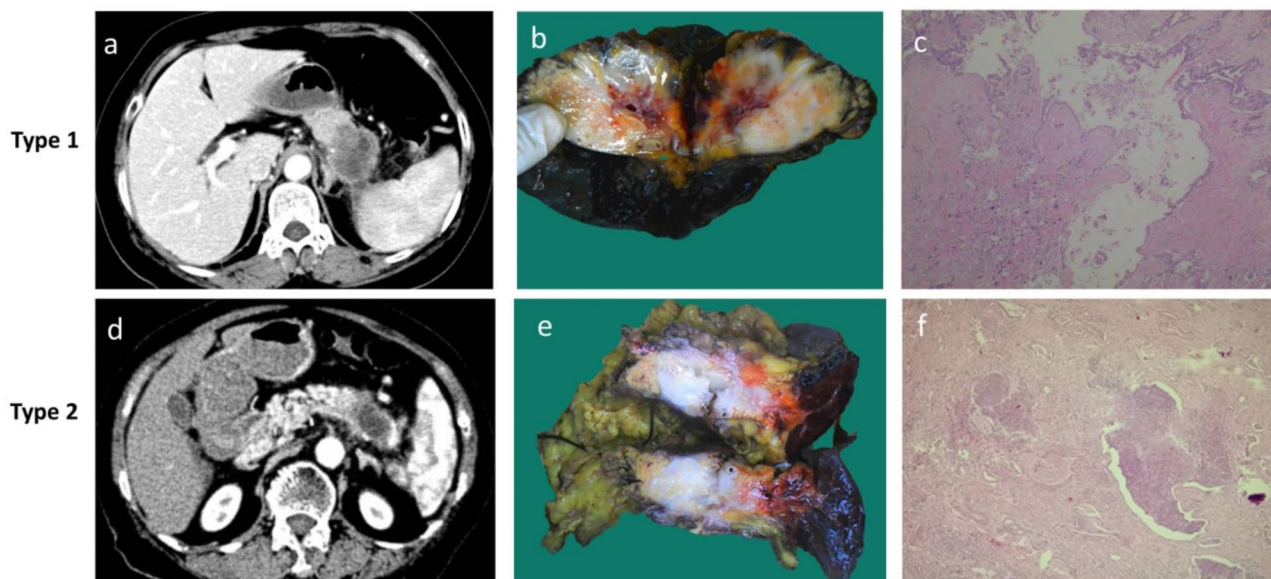


**Fig. 6** A 60-year-old woman with poorly differentiated PDAC: **a** CT post-contrast image showing a mildly bulging lesion in the pancreatic tail, which demonstrates hypoattenuating enhancement during the venous phase with an eccentric small cystic lesion. **b** Macroscopic photography of the specimen reveals a tan-white solid mass with an intratumoral small cyst and areas of hemorrhage. **c** Microscopic image (hematoxylin and eosin; original magnification  $\times 40$ ) shows an irregular, large duct-type gland with partial shedding of the epithelium. A 75-year-old woman diagnosed with moderately differentiated pancreatic cancer: **d** CT post-contrast image displaying a mildly bulging mass with a large intratumoral cyst in the pancreatic body/tail. **e** Macroscopic specimen reveals an irregular cavity at the center of the mass. **f** Microscopic image (hematoxylin & eosin; original magnification  $\times 40$ ) demonstrates focal coagulation necrosis

**Table 2** Histopathologic characteristics of surgically resected pancreatic adenocarcinomas with cystic lesions

Data	Total (n = 23)	Type I (n = 13)	Type II (n = 3)	Type III (n = 7)
Size*, cm	5.5 ± 2.3	5.6 ± 2.5	6.8 ± 1.9	4.8 ± 2.2
Tumor stage				
T1	1 (4.3%)	0 (0)	0 (0)	1 (14.3%)
T2	6 (26.1%)	4 (30.8%)	0 (0)	2 (28.6%)
T3	14 (60.1%)	8 (61.5%)	3 (100%)	3 (42.8%)
T4	2 (8.7%)	1 (7.7%)	0 (0)	1 (14.3%)
Node satge				
N0	18 (78.3%)	9 (69.2%)	3 (100%)	6 (85.7%)
N1	5 (21.7%)	4 (30.8%)	0 (0)	1 (14.3%)
N2	0 (0)	0 (0)	0 (0)	0 (0)
Histological grading				
Well differentiated	0 (0)	0 (0)	0 (0)	0 (0)
Moderately differentiated	14 (60.9%)	7 (53.8%)	1 (33.3%)	6 (85.7%)
Poorly differentiated	9 (39.1%)	6 (46.2%)	2 (66.7%)	1 (14.3%)
Peripancreatic infiltration				
perineural invasion	19 (82.6%)	12 (92.3%)	2 (66.7%)	5 (71.4%)
fat invasion	14 (60.9%)	6 (46.2%)	2 (66.7%)	6 (85.7%)
Macroscopic cyst-like cavities				
Absence	8 (34.8%)	5 (38.5%)	1 (33.3%)	2 (28.6%)
Presence	15 (65.2%)	8 (61.5%)	2 (66.7%)	5 (71.4%)
Microscopy appearance				
Absence	9 (39.1%)	3 (23%)	2 (66.7%)	4 (57.1%)
Presence	14 (60.9%)	10 (77%)	1 (33.3%)	3 (42.9%)
Large duct-type	5 (35.7%)	3 (30%)	0 (0)	2 (66.7%)
Coagulative necrosis	6 (42.9%)	4 (40%)	1 (100%)	1 (33.3%)
Extracellular mucin deposit	2 (14.2%)	2 (20%)	0 (0)	0 (0)
Large duct-type concomitant extracellular mucin deposition	1 (7.1%)	1 (10%)	0 (0)	0 (0)

Note—Except for size, Data are in number of occurrences. Data in parentheses represent percentages

\*Data are expressed as mean ± standard deviation

So far, there is no universally accepted standard for defining cystic features in PDACs on CT imaging, previous studies have predominantly relied on subjective visual descriptors, such as “cyst-like features,” “obvious low attenuation,” or “hypodense cystic lesions,” sometimes compared to “gallbladder density”. Additionally, the heterogeneous composition of cystic fluid complicates the accurate identification of cystic degeneration in PDACs. For instance, Adsay et al. [21] documented instances where lesions initially identified as radiologically evident cysts, presumed to be “pseudocysts,” were subsequently found to consist of solid tissue upon pathological examination. In our series, we observed six cases of PDACs with cyst-appearing lesions on DCE-CT, four of which were ultimately pathologically confirmed as solid masses without cystic lesions. Retrospective analysis revealed that the CT values of all six lesions exceeded 20 HU and showed no enhancement on DCE-CT. Consequently, our study implemented a stringent inclusion criterion for defining cystic lesions, setting the average CT values of cystic lesions ranging between -10 HU and 20 HU, consistent with parameters utilized in prior

studies [14]. This approach ensures higher accuracy and reproducibility of defining cystic lesions in the context of PDAC.

Secondary signs are crucial diagnostic indicators in the detection of PDAC. Our findings are consistent with previous research that highlights the significance of pancreatic duct abnormalities in the diagnosis of PDAC. However, we also acknowledge the importance of considering PDACs that may occur in the absence of secondary signs. As noted by Tamada et al. [24], cases of PDAC without secondary signs can be explained by anatomical and histopathological factors. In our cohort, five cases were initially misdiagnosed for lack of secondary signs, four cases demonstrated exophytic growth, extending towards the dorsal side of the pancreas, one of which located in the uncinata. The remaining one involved nearly the entire pancreas. These growth patterns may be attributable to the exophytic nature of the tumors, which develop away from the pancreatic duct, or to the involvement of the entire main pancreatic duct.

In our cohort of surgically resected PDAC cases, the average pathological size was 5.5 cm, with all tumors

being moderately or poorly differentiated, and no well-differentiated cases were observed. Additionally, peripancreatic invasion was notably more common, suggesting a potentially poor prognosis [25]. Interestingly, we found that PDACs with associated with peritumoral cystic lesions in our group are more frequently characterized by fat infiltration and moderate differentiation. Furthermore, coagulative necrosis and large duct-type cystic changes were relatively common under microscopic examination, while extracellular mucin deposits were less frequently observed. Our study also identified three cases exhibiting multiple large cystic structures on DCE-CT, which resembled the multiple large cystic phenotype described by Nitta et al. [7]. In our study, most of the CT findings (PDAC tumor entity and accompanying cystic lesions) were consistent with the pathological changes. However, CT findings did indeed show discrepancies with the final pathology in some cases. For example, in 2 cases of Type 3 tumors, the CT images of tumor entity of pancreatic parenchyma did not show typical cystic changes, while microscopic examination revealed coagulative necrosis and large duct features, which may be related to the relatively low number of cystic large ducts.

Isoattenuating enhanced PDACs have been recognized as a distinct subtype, as reported in the literature [15, 26, 27], which is one of the primary causes of missed diagnosis or misdiagnosis [3]. In our study, four cases of isoattenuating enhanced PDACs were misdiagnosed as neuroendocrine carcinoma. Upon reviewing the imaging characteristics of these cases, two were relatively small, consistent with previously reported cases [15, 26, 27]. The other two cases demonstrated larger size with higher T-grade, and the presence of intratumoral proliferation of small arteries were found in these two tumors. Previous studies have indicated that the presence of intratumoral arterioles is associated with poorer prognosis in PDACs [28], suggesting that monitoring intratumoral arterioles may serve as a potential prognostic factor in the management of PDACs.

PDACs with cystic lesions can mimic cystic neoplasms on imaging. In our study, one case was missed diagnosed (2.5%), while 14 cases (35%) were misdiagnosed. The majority of type 2 cases were misdiagnosed as other cystic malignancies of the pancreas (83.3%), possibly due to the large size of the cystic components. It is noteworthy that several pancreatic neoplastic and non-neoplastic entities may mimic the imaging appearance of PDAC with cystic lesions. (1) Pancreatic neuroendocrine tumors (PNETs) may demonstrate atypical hypovascularity masses [29] with cystic degeneration, making them difficult to distinguish from PDAC with cystic lesions. However, PNETs typically exhibit more well-defined margins and less severe upstream pancreatic ductal dilatation, and CT attenuation values during the arterial and portal venous

phase may help differentiate them from PDAC [30]; (2) Solid pseudopapillary tumors (SPTs) are indolent pancreatic neoplasms with malignant potential, predominantly occurring in young women. Imaging features such as the “floating cloud sign” are more commonly seen in SPTs rather than PDACs [31]; (3) Serous cystic neoplasms (SCNs) and mucinous cystic neoplasms (MCNs) with thick enhancing cyst wall or solid components can be difficult to distinguish with PDAC, SCA is among the few hypervascular cystic pancreatic neoplasms, and MCNs are seen nearly exclusively in women [32, 33]; (4) Mass-forming pancreatitis (MFP) can mimic PDAC when presenting as a hypoattenuating mass. Key differentiating features include a clinical history of pancreatitis and the “duct-penetrating sign” are more commonly associated with MFP [34].

This study has several limitations. First, the sample size is relatively small due to the rarity of PDACs with cystic lesions, therefore, it is difficult to collect many cases in a short time period. Future studies will focus on gathering additional cases to provide a more comprehensive and detailed analysis of the radiological-pathological correlation. Second, while CT is the preferred first-line imaging modality for PDAC, and this study mainly focused on the CT imaging features of PDACs with cystic lesions, we acknowledge that MRI may be better suited for visualizing small cystic foci, and future studies could integrate MRI findings for further analysis. Third, based on our limited experience, we defined the CT value of cystic lesions as ranging from  $-10$  HU to  $20$  HU, mainly to avoid misclassifying solid PDACs as having cystic features. However, this criterion may exclude a small number of cystic lesions with complex components (e.g., high protein or bleeding). Fourth, this study did not investigate the prognosis of PDACs with different types of cystic lesions, and prospective follow-up studies are needed to clarify the clinical significance of these subtypes.

In conclusion, our study classifies PDACs with cystic lesions into three types based on their morphological characteristics observed on CT. We found that PDACs with cystic lesions are more common in the pancreatic body and tail, with histopathological findings of coagulative necrosis and large duct-type cystic changes. Type 2 cases exhibit a high misdiagnosis rate, particularly due to large intratumoral cystic components, which indicated that although PDACs with cystic lesions are relatively rare, their possibility should be considered in the differential diagnosis when cystic lesions of the pancreas are observed on imaging.

#### Abbreviations

CA 19–9	Carbohydrate antigen 19–9
CT	Computed tomography
DCE-CT	Dynamic contrast-enhanced computed tomography
MR	Magnetic resonance

PDAC Pancreatic ductal adenocarcinoma

## Supplementary Information

The online version contains supplementary material available at <https://doi.org/10.1186/s12880-025-01586-4>.

Supplementary Material 1

### Acknowledgements

We would like to acknowledge the hard and dedicated work of all the staff in the study.

### Author contributions

Conception and design of the research: Jing Chen, Ruimeng Yang, Acquisition of data: Jing Chen, Ling Liu, Zhe Wu, Yuan Yuan, Qi Wu. Analysis and interpretation of the data: Jing Chen, Ruimeng Yang, Shengsheng Lai. Statistical analysis: Jing Chen, Writing of the manuscript: Jing Chen, Ruimeng Yang. Critical revision of the manuscript for intellectual content: Jing Chen, Ruimeng Yang. All authors read and approved the final draft.

### Funding

This work was funded by the National Natural Science Foundation of China (82371908, 81971574), the Guangdong Natural Science Foundation (2024A1515012177), the Guangdong Basic and Applied Basic Research Foundation (2021A1515220060), Guangzhou Key Laboratory of Molecular Imaging and Clinical Translational Medicine (202201020376), Medical Science and Technology Research Project of Guangdong Province (A2024637).

### Data availability

The datasets used and/or analyzed during the current study are available from the corresponding author on reasonable request.

### Declarations

#### Ethics approval and consent to participate

This study was a retrospective study and was approved by the ethics committee of Yichang Central People's Hospital, Hubei, China (Approval numbers: No. 2023-049-01). The requirement for informed consent was waived by the Medical Ethics Committee. Authors confirm that all methods were carried out in accordance with relevant guidelines and regulations.

#### Consent for publication

Not applicable.

#### Competing interests

The authors declare no competing interests.

#### Clinical trial number

Not applicable.

Received: 22 October 2024 / Accepted: 10 February 2025

Published online: 14 March 2025

### References

- Elbanna KY, Jang HJ, Kim TK. Imaging diagnosis and staging of pancreatic ductal adenocarcinoma: a comprehensive review. *Insights Imaging*. 2020;11(1):58.
- Yang J, Xu R, Wang C, Qiu J, Ren B, You L. Early screening and diagnosis strategies of pancreatic cancer: a comprehensive review. *Cancer Commun (Lond)*. 2021;41(12):1257–74.
- Gong XH, Xu JR, Qian LJ. Atypical and uncommon CT and MR imaging presentations of pancreatic ductal adenocarcinoma. *Abdom Radiol (NY)*. 2021;46(9):4226–37.
- Paik KY, Choi SH, Heo JS, Choi DW. Solid tumors of the pancreas can put on a mask through cystic change. *World J Surg Oncol*. 2011;9:79.
- Kosmahl M, Pauser U, Anlauf M, Klöppel G. Pancreatic ductal adenocarcinomas with cystic features: neither rare nor uniform. *Mod Pathol*. 2005;18(9):1157–64.
- H'ng MW, Kwek JW, Teo CH, Cheong DM. Cystic degeneration of ductal adenocarcinoma of the pancreatic tail. *Singap Med J*. 2009;50(3):e91–3.
- Nitta T, Mitsuhashi T, Hatanaka Y, Hirano S, Matsuno Y. Pancreatic ductal adenocarcinomas with multiple large cystic structures: a clinicopathologic and immunohistochemical study of seven cases. *Pancreatol*. 2013;13(4):401–8.
- Yoon SE, Byun JH, Kim KA, et al. Pancreatic ductal adenocarcinoma with intratumoral cystic lesions on MRI: correlation with histopathological findings. *Br J Radiol*. 2010;83(988):318–26.
- Youn SY, Rha SE, Jung ES, Lee IS. Pancreas ductal adenocarcinoma with cystic features on cross-sectional imaging: radiologic-pathologic correlation. *Diagn Interv Radiol*. 2018;24(1):5–11.
- Bagci P, Andea AA, Basturk O, Jang KT, Erbarur I, Adsay V. Large duct type invasive adenocarcinoma of the pancreas with microcystic and papillary patterns: a potential microscopic mimic of non-invasive ductal neoplasia. *Mod Pathol*. 2012;25(3):439–48.
- Hara A, Yamada Y, Fukuzawa K, et al. Honeycomb appearance in large-duct type pancreatic ductal adenocarcinoma: case report with radiologic-pathologic correlation. *Radiol Case Rep*. 2022;17(9):3439–45.
- Sato H, Liss AS, Mizukami Y. Large-duct pattern invasive adenocarcinoma of the pancreas—a variant mimicking pancreatic cystic neoplasms: a minireview. *World J Gastroenterol*. 2021;27(23):3262–78.
- Vullierme MP. Imaging classification of pancreatic ductal adenocarcinoma with histological large duct pattern: beware of serous cystadenoma. *Eur Radiol*. 2024;34(11):7013–4.
- Chen X, Yu Z, Wang J, et al. Opportunistic detection for pancreatic cystic lesions during chest multidetector CT scans for lung cancer screening. *Cancer Manag Res*. 2021;13:7559–68.
- Kim JH, Park SH, Yu ES, et al. Visually isoattenuating pancreatic adenocarcinoma at dynamic-enhanced CT: frequency, clinical and pathologic characteristics, and diagnosis at imaging examinations. *Radiology*. 2010;257(1):87–96.
- Toshima F, Watanabe R, Inoue D, et al. CT abnormalities of the pancreas associated with the subsequent diagnosis of clinical stage I pancreatic ductal adenocarcinoma more than 1 year later: a case-control study. *AJR Am J Roentgenol*. 2021;217(6):1353–64.
- van Roessel S, Kasumova GG, Verheij J, et al. International validation of the eighth edition of the American Joint Committee on Cancer (AJCC) TNM staging system in patients with resected pancreatic cancer. *JAMA Surg*. 2018;153(12):e183617.
- Basturk O, Coban I, Adsay NV. Pancreatic cysts: pathologic classification, differential diagnosis, and clinical implications. *Arch Pathol Lab Med*. 2009;133(3):423–38.
- Garcea G, Ong SL, Rajesh A, et al. Cystic lesions of the pancreas. A diagnostic and management dilemma. *Pancreatol*. 2008;8(3):236–51.
- Kosmahl M, Pauser U, Peters K, et al. Cystic neoplasms of the pancreas and tumor-like lesions with cystic features: a review of 418 cases and a classification proposal. *Virchows Arch*. 2004;445(2):168–78.
- Volkman Adsay N. Cystic lesions of the pancreas. *Mod Pathol*. 2007;20(Suppl 1):S71–93.
- Lv P, Mahyoub R, Lin X, Chen K, Chai W, Xie J. Differentiating pancreatic ductal adenocarcinoma from pancreatic serous cystadenoma, mucinous cystadenoma, and a pseudocyst with detailed analysis of cystic features on CT scans: a preliminary study. *Korean J Radiol*. 2011;12(2):187–95.
- Kang JD, Clarke SE, Costa AF. Factors associated with missed and misinterpreted cases of pancreatic ductal adenocarcinoma. *Eur Radiol*. 2021;31(4):2422–32.
- Tamada T, Ito K, Kanomata N, et al. Pancreatic adenocarcinomas without secondary signs on multiphase multidetector CT: association with clinical and histopathologic features. *Eur Radiol*. 2016;26(3):646–55.
- De Robertis R, Beleù A, Cardobi N, et al. Correlation of MR features and histogram-derived parameters with aggressiveness and outcomes after resection in pancreatic ductal adenocarcinoma. *Abdom Radiol (NY)*. 2020;45(11):3809–18.
- Psar R, Urban O, Cerna M, Rohan T, Hill M. Improvement of the diagnosis of isoattenuating pancreatic carcinomas by defining their characteristics on contrast enhanced computed tomography and endosonography with fine-needle aspiration (EUS-FNA). *Diagnostics (Basel)*. 2021. 11(5).
- Yoon SH, Lee JM, Cho JY, et al. Small ( $\leq 20$  mm) pancreatic adenocarcinomas: analysis of enhancement patterns and secondary signs with multiphase multidetector CT. *Radiology*. 2011;259(2):442–52.

28. Hori S, Shimada K, Ino Y, et al. Macroscopic features predict outcome in patients with pancreatic ductal adenocarcinoma. *Virchows Arch.* 2016;469(6):621–34.
29. Karmazanovsky G, Belousova E, Schima W, Glotov A, Kalinin D, Kriger A. Nonhypervascular pancreatic neuroendocrine tumors: spectrum of MDCT imaging findings and differentiation from pancreatic ductal adenocarcinoma. *Eur J Radiol.* 2019;110:66–73.
30. Ren S, Chen X, Wang Z, et al. Differentiation of hypovascular pancreatic neuroendocrine tumors from pancreatic ductal adenocarcinoma using contrast-enhanced computed tomography. *PLoS ONE.* 2019;14(2):e0211566.
31. Ren S, Qian LC, Lv XJ, et al. Comparison between solid pseudopapillary neoplasms of the pancreas and pancreatic ductal adenocarcinoma with cystic changes using computed tomography. *World J Radiol.* 2024;16(6):211–20.
32. Kang JS, Kim HJ, Choi YJ, et al. Clinicoradiological features of resected serous cystic neoplasms according to morphological subtype and preoperative tentative diagnosis: can radiological characteristics distinguish serous cystic neoplasms from other lesions. *Ann Surg Treat Res.* 2020;98(5):247–53.
33. Miller FH, Lopes Vendrami C, Recht HS, et al. Pancreatic cystic lesions and malignancy: assessment, guidelines, and the field defect. *Radiographics.* 2022;42(1):87–105.
34. Ren S, Zhang J, Chen J, et al. Evaluation of texture analysis for the differential diagnosis of mass-forming pancreatitis from pancreatic ductal adenocarcinoma on contrast-enhanced CT images. *Front Oncol.* 2019;9:1171.

### Publisher's note

Springer Nature remains neutral with regard to jurisdictional claims in published maps and institutional affiliations.